Advances in Engineering Software 59 (2013) 53–70

Contents lists available at SciVerse ScienceDirect

Advances in Engineering Software

journal homepage: www.elsevier.com/locate/advengsoft

A new optimization method: Dolphin echolocation

A. Kaveh *, N. Farhoudi

Centre of Excellence for Studies in Structural Engineering, School of Civil Engineering, Iran University of Science and Technology, Tehran-16, Iran

ARTICLE INFO

Article history:
Received 10 September 2012
Received in revised form 12 March 2013
Accepted 24 March 2013
Available online 23 April 2013

Keywords:
Optimization
Meta-heuristic
Dolphin echolocation
Optimal design
Trusses
Frames

ABSTRACT

Nature has provided inspiration for most of the man-made technologies. Scientists believe that dolphins are the second to humans in smartness and intelligence. Echolocation is the biological sonar used by dolphins and several kinds of other animals for navigation and hunting in various environments. This ability of dolphins is mimicked in this paper to develop a new optimization method. There are different meta-heuristic optimization methods, but in most of these algorithms parameter tuning takes a considerable time of the user, persuading the scientists to develop ideas to improve these methods. Studies have shown that meta-heuristic algorithms have certain governing rules and knowing these rules helps to get better results. Dolphin echolocation takes advantages of these rules and outperforms many existing optimization methods, while it has few parameters to be set. The new approach leads to excellent results with low computational efforts.

1. Introduction

The recent generation of the optimization methods is meta-heuristics that are proposed to solve complex problems. Every meta-heuristic method consists of a group of search agents that explore the feasible region based on both randomization and some specified rules [1]. The rules are usually inspired by the laws of natural phenomena. Genetic Algorithm (GA) proposed by Holland [2] and Goldberg [3] is inspired by Darwin's theory about biological evolutions. Particle swarm optimization (PSO) proposed by Eberhart and Kennedy [4] simulates social behavior, and it is inspired by the movement of organisms in a bird flock or fish school. Truss optimization with dynamic constraints using a particle swarm algorithm can be found in the work of Gomes [5]. Ant Colony Optimization (ACO) formulated by Dorigo et al. [6] imitates foraging behavior of ant colonies. Many other natural-inspired algorithms such as Simulated Annealing (SA) proposed by Kirkpatrick et al. [7], Harmony Search (SA) presented by Geem et al. [8], Gravitational Search Algorithm (GSA) proposed by Rashedi et al. [9], Big Bang–Big Crunch algorithm (BB–BC) proposed by Erol and Eksin [10], and improved by Kaveh and Talatahari [11]. Due to their good performance and ease of implementation, these methods have been widely applied to various problems in different fields of science and engineering. Structural optimization is one of the active branches of the applications of optimization algorithms [12–15]. One of the most recent meta-heuristic algorithms is the Charged System Search (CSS) proposed by Kaveh and Talatahari [16] that uses the electric laws of physics and the Newtonian laws of mechanics to guide the Charged Particles (CPs) to explore the locations of the optimum. Bat-inspired algorithm introduced by Yang [17] is another recent meta-heuristic algorithm which mimics the behavior of bats in detecting prey.

Dolphin echolocation is a new optimization method which is presented in this paper. This method mimics strategies used by dolphins for their hunting process. Dolphins produce a kind of voice called *sonar* to locate the target, doing this dolphin change sonar to modify the target and its location. Dolphin echolocation is depicted in Fig. 1. This fact is mimicked here as the main feature of the new optimization method.

After this introduction, Section 2 presents the dolphin's echolocation in nature. Section 3 introduces dolphin echolocation algorithm, Section 4 presents structural optimization problems to be solved. This follows by Section 5 which includes some numerical examples from truss and frame structures. The last section is devoted to concluding remarks indicating the capabilities of the new method in comparison to some other meta-heuristic algorithms like GA, ACO, PSO, BB, HS, SA, and CSS.

2. Dolphin echolocation in nature

The term "echolocation" was initiated by Griffin [18] to describe the ability of flying bats to locate obstacles and preys by listening to echoes returning from high-frequency clicks that they emitted. Echolocating animals include some mammals and a few birds. The best studied echolocation in marine mammals is that of the bottlenose dolphins, Au [19].

A dolphin is able to generate sounds in the form of clicks. Frequency of these clicks is higher than that of the sounds used for

* Corresponding author.
E-mail address: alikaveh@iust.ac.ir (A. Kaveh).

0965-9978/$ - see front matter © 2013 Elsevier Ltd. All rights reserved.
http://dx.doi.org/10.1016/j.advengsoft.2013.03.004

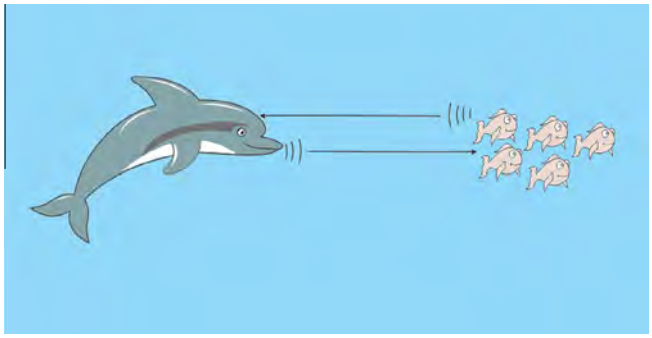

Fig. 1. A real dolphin catching its prey.

Table 1
An example for calculation of the CF [1].

	Element 1	Element 2	Element 3	Element 4
Answer 1	5	41	22	15
Answer 2	3	36	22	17
Answer 3	4	39	25	16
Answer 4	3	42	22	17
Answer 5	3	41	22	19
Modal answer	3	41	22	17
Frequency of the modal answer	3	2	4	2
Proportion of the modal answer among all answers	60%	40%	80%	40%
CF	55%			

communication and differs between species. When the sound strikes an object, some of the energy of the sound-wave is reflected back towards the dolphin. As soon as an echo is received, the dolphin generates another click. The time lapse between click and echo enables the dolphin to evaluate the distance from the object; the varying strength of the signal as it is received on the two sides of the dolphin's head enabling him to evaluate the direction. By continuously emitting clicks and receiving echoes in this way, the dolphin can track objects and home in on them, May [20]. The clicks are directional and are for echolocation, often occurring in a short series called a click train. The click rate increases when approaching an object of interest, Au [19].

Though bats also use echolocation, however, they differ from dolphins in their sonar system. Bats use their sonar system at short ranges of up to approximately 3–4 m, whereas dolphins can detect their targets at ranges varying from a few tens of meters to over a hundred meters. Many bats hunt for insects that dart rapidly to-and-fro, making it very different from the escape behavior of a fish chased by dolphin. The speed of sound in air is about one fifth of that of water, thus the information transfer rate during sonar transmission for bats is much shorter than that of the dolphins. These and many other differences in environment and prey require totally different types of sonar system, which naturally makes a direct comparison difficult [19,21].

3. Dolphin echolocation optimization

3.1. Introduction to dolphin echolocation

Regarding an optimization problem, it can be understood that echolocation is similar to optimization in some aspects; the process of foraging preys using echolocation in dolphins is similar to finding the optimum answer of a problem.

As mentioned in the previous part, dolphins initially search all around the search space to find the prey. As soon as a dolphin approaches the target, the animal restricts its search, and incrementally increases its clicks in order to concentrate on the location.

The method simulates dolphin echolocation by limiting its exploration proportional to the distance from the target. For making the relationship much clear, consider an optimization problem. Two phases can be identified: in the first phase the algorithm explores all around the search space to perform a global search, therefore it should look for unexplored regions. This task is carried out by exploring some random locations in the search space, and in the second phase it concentrates on investigation around better results achieved from the previous stage. These are obvious inherent characteristics of all meta-heuristic algorithms. An efficient method is presented in Ref. [1] for controlling the value of the randomly

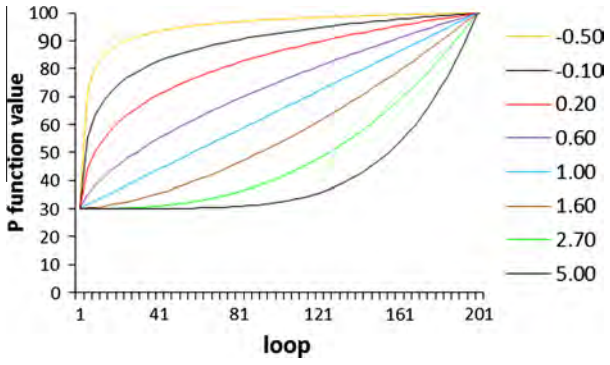

Fig. 2. Sample convergence curves, using Eq. (1) for different values for power [1].

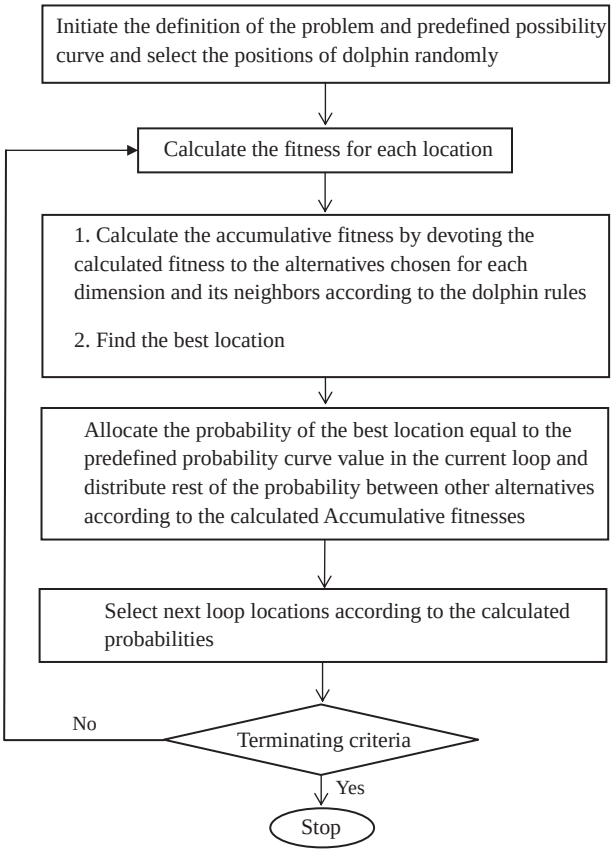

Fig. 3. The flowchart of the DE algorithm.

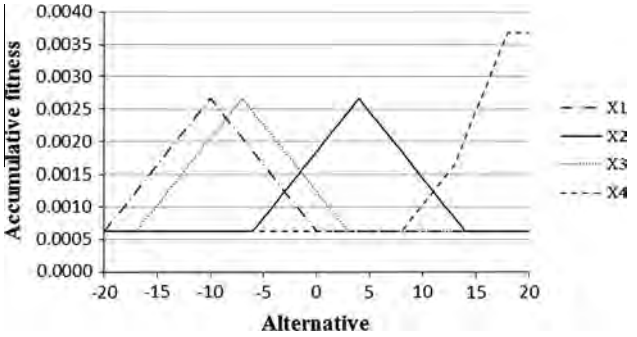

Fig. 4. Accumulative fitness resulted from sample location of the mathematical example.

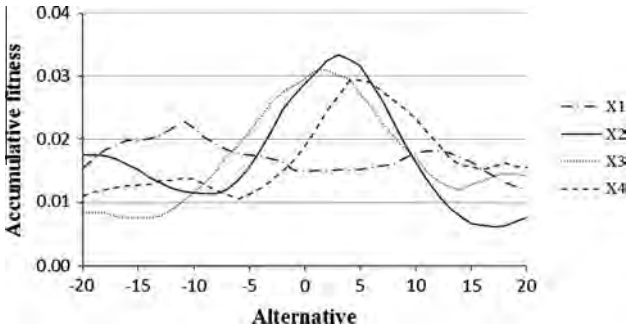

Fig. 5. Accumulative fitness of all four variables in the first loop of DE in mathematical example.

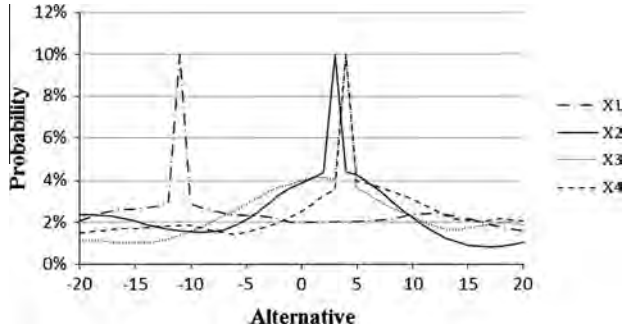

Fig. 6. Probability curve of all four variables in the first loop of DE in mathematical example.

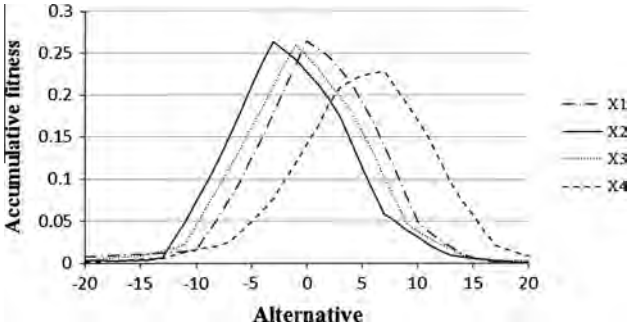

Fig. 7. Accumulative fitness of all four variables in the 4th loop of DE in of mathematical example.

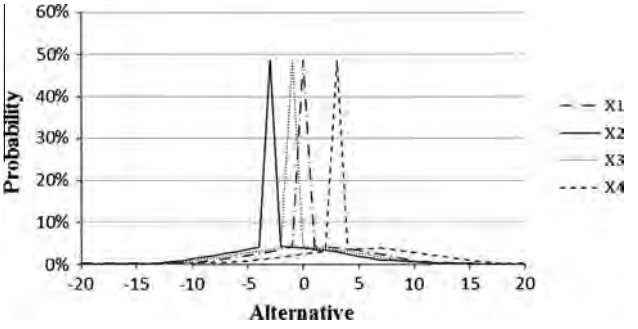

Fig. 8. Probability curve of all four variables in the 4th loop of DE in mathematical example.

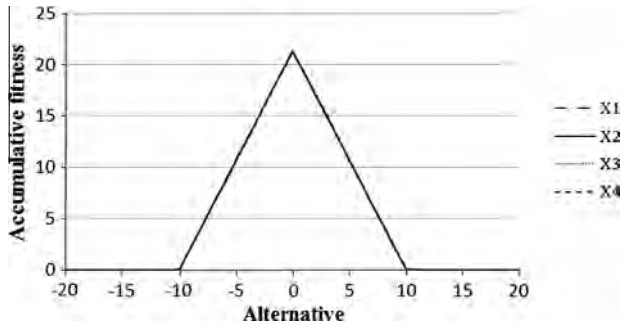

Fig. 9. Accumulative fitness of all four variables in the 8th loop of DE in of mathematical example.

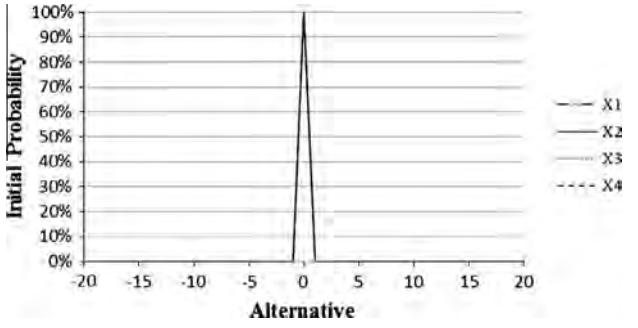

Fig. 10. Probability curve of all four variables in the 8th loop of DE in mathematical example.

created answers in order to set the ratio of the results to be achieved in phase 1 to phase 2.

By using dolphin echolocation (DE) algorithm, the user would be able to change the ratio of answers produced in phase 1 to the answers produces in phase 2 according to a predefined curve. In other words, global search, changes to a local one gradually in a user defined style.

The user defines a curve on which the optimization convergence should be performed, then the algorithm sets its parameters in order to be able to follow the curve. The method works with the likelihood of occurrence of the best answer in comparison to the others. In other words, for each variable there are different alternatives in the feasible region, in each loop the algorithm defines the possibility of choosing the best so far achieved alternative according to the user determined convergence curve. By using this curve, the convergence criterion is dictated to the algorithm, and then the convergence of the algorithm becomes less parameter dependent.

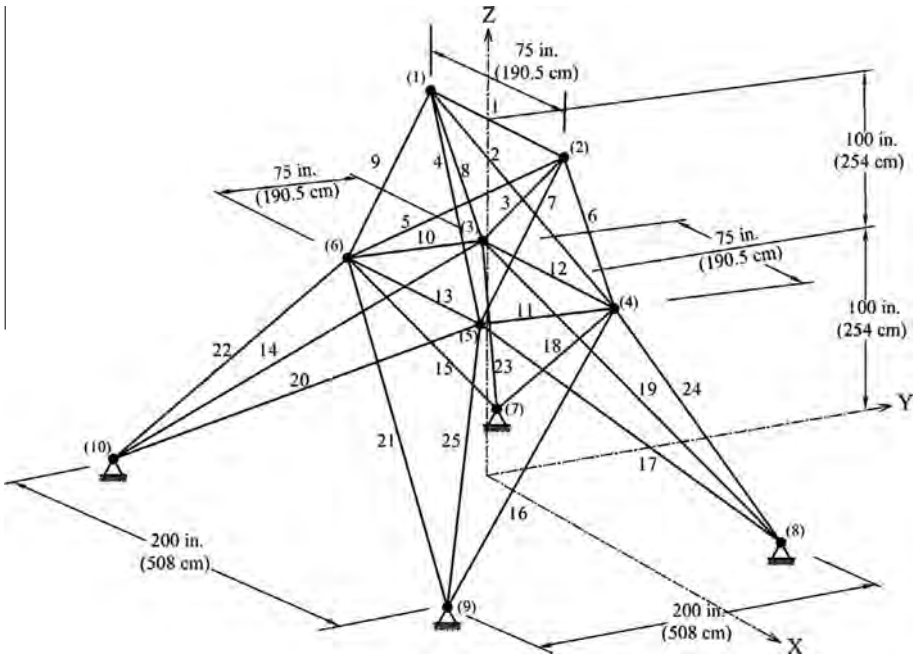

Fig. 11. A 25-bar spatial truss.

Table 2
The available cross-section areas of the AISC code.

No.	in.^{2}	mm^2	No.	in.^{2}	mm^2
1	0.111	(71.613)	33	3.840	(2477.414)
2	0.141	(90.968)	34	3.870	(2496.769)
3	0.196	(126.451)	35	3.880	(2503.221)
4	0.250	(161.290)	36	4.180	(2696.769)
5	0.307	(198.064)	37	4.220	(2722.575)
6	0.391	(252.258)	38	4.490	(2896.768)
7	0.442	(285.161)	39	4.590	(2961.284)
8	0.563	(363.225)	40	4.800	(3096.768)
9	0.602	(388.386)	41	4.970	(3206.445)
10	0.766	(494.193)	42	5.120	(3303.219)
11	0.785	(506.451)	43	5.740	(3703.218)
12	0.994	(641.289)	44	7.220	(4658.055)
13	1.000	(645.160)	45	7.970	(5141.925)
14	1.228	(792.256)	46	8.530	(5503.215)
15	1.266	(816.773)	47	9.300	(5999.988)
16	1.457	(939.998)	48	10.850	(6999.986)
17	1.563	(1008.385)	49	11.500	(7419.430)
18	1.620	(1045.159)	50	13.500	(8709.660)
19	1.800	(1161.288)	51	13.900	(8967.724)
20	1.990	(1283.868)	52	14.200	(9161.272)
21	2.130	(1374.191)	53	15.500	(9999.980)
22	2.380	(1535.481)	54	16.000	(10322.560)
23	2.620	(1690.319)	55	16.900	(10903.204)
24	2.630	(1696.771)	56	18.800	(12129.008)
25	2.880	(1858.061)	57	19.900	(12838.684)
26	2.930	(1890.319)	58	22.000	(14193.520)
27	3.090	(1993.544)	59	22.900	(14774.164)
28	1.130	(729.031)	60	24.500	(15806.420)
29	3.380	(2180.641)	61	26.500	(17096.740)
30	3.470	(2238.705)	62	28.000	(18064.480)
31	3.550	(2290.318)	63	30.000	(19354.800)
32	3.630	(2341.931)	64	33.500	(21612.860)

The curve can be any smooth ascending curve but there are some recommendations for it, which will be discussed later.

Previously it has been shown that there is a unified method for parameter selection in meta-heuristics [1]. In the latter paper, an index called the convergence factor was presented. A *Convergence Factor* (*CF*) is defined as the average possibility of the elitist answer. As an example, if the aim is to devote some steel profiles to a structure that has four elements, then in the first step, frequency of modal profile of each element should be defined. *CF* is the mean of these frequencies. Table 1 illustrates an example of calculating the *CF* for a structure containing four elements.

3.2. Dolphin echolocation algorithm

Before starting optimization, search space should be sorted using the following rule:

Search space ordering: For each variable to be optimized during the process, sort alternatives of the search space in an ascending or descending order. If alternatives include more than one characteristic, perform ordering according to the most important one. Using this method, for variable j, vector A_j of length LA_j is created which contains all possible alternatives for the jth variable putting these vectors next to each other, as the columns of a matrix, the *Matrix Alternatives*$_{MA*NV}$ is created, in which MA is $\max(LA_j)_{j=1:NV}$; with NV being the number of variables.

Moreover, a curve according to which the convergence factor should change during the optimization process, should be assigned. Here, the change of *CF* is considered to be according to the following curve:

$$PP(Loop_i) = PP_1 + (1 - PP_1)\frac{Loop_i^{Power} - 1}{(LoopsNumber)^{Power} - 1} \quad (1)$$

PP is the predefined probability, PP_1 the convergence factor of the first loop in which the answers are selected randomly, $Loop_i$ the number of the current loop, and *Power* is the degree of the curve. As it can be seen, the curve in Eq. (1) is of *Power* degree.

Loops Number: Number of loops in which the algorithm should reach to the convergence point. This number should be chosen by the user according to the computational effort that can be afforded for the algorithm.

Fig. 2 shows the variation of PP by the changes of the *Power*, using the proposed formula, Eq. (1).

Table 3
Loading conditions for the 25-bar spatial truss.

Node	Case 1			Case 2		
	P_X kips (kN)	P_Y kips (kN)	P_Z kips (kN)	P_X kips (kN)	P_Y kips (kN)	P_Z kips (kN)
1	0.0	20.0 (89)	−5.0 (22.25)	1.0 (4.45)	10.0 (44.5)	−5.0 (22.25)
2	0.0	−20.0 (89)	−5.0 (22.25)	0.0	10.0 (44.5)	−5.0 (22.25)
3	0.0	0.0	0.0	0.5 (2.22)	0.0	0.0
6	0.0	0.0	0.0	0.5 (2.22)	0.0	0.0

Table 4
Optimal design comparison for the 25-bar spatial truss (Case 1).

Element group		Optimal cross-sectional areas (in.^{2})								
		Wu and Chow [22]	Lee and Geem [23]	Li et al. [24]			Kaveh and Talatahari [25] HPSACO		Present work	
		GA	HS	PSO	PSOPC	HPSO	in.^{2}	cm^2	in.^{2}	cm^2
1	A1	0.40	0.01	0.01	0.01	0.01	0.01	0.07	0.01	0.07
2	A_2–A_5	2.00	2.00	2.00	2.00	2.00	1.60	10.32	1.60	10.32
3	A_6–A_9	3.60	3.60	3.60	3.60	3.60	3.20	20.65	3.20	20.65
4	A_{10}–A_{11}	0.01	0.01	0.01	0.01	0.01	0.01	0.07	0.01	0.07
5	A_{12}–A_{13}	0.01	0.01	0.40	0.01	0.01	0.01	0.07	0.01	0.07
6	A_{14}–A_{17}	0.80	0.80	0.80	0.80	0.80	0.80	5.16	0.80	5.16
7	A_{18}–A_{21}	2.00	1.60	1.60	1.60	1.60	2.00	12.90	2.00	12.90
8	A_{22}–A_{25}	2.40	2.40	2.40	2.40	2.40	2.40	15.48	2.40	15.48
Weight (lb)		563.52	560.59	566.44	560.59	560.59	551.6	250.2 kg	551.6	250.2 kg

The flowchart of the algorithm is shown in Fig. 3. The main steps of dolphin echolocation (DE) for discrete optimization are as follows:

1. Initiate *NL* locations for a dolphin randomly.

This step contains creating L_{NL*NV} matrix, in which *NL* is the number of locations and *NV* is the number of variables (or dimension of each location).

2. Calculate the *PP* of the loop using Eq. (1).
3. Calculate the fitness of each location.

Fitness should be defined in a manner that the better answers get higher values. In other words the optimization goal should be to maximize the fitness.

4. Calculate the accumulative fitness according to dolphin rules as follows:

(a)
for i = 1 to the number of locations
  for j = 1 to the number of variables
    find the position of $L(i,j)$ in jth column of the
  Alternatives matrix and name it as A.
    for k = -R_e to R_e

$$AF_{(A+k)j} = \frac{1}{R_e} * (R_e - |k|)Fitness(i) + AF_{(A+k)j} \quad (2)$$

    end
  end
end

where $AF_{(A+k)j}$ is the accumulative fitness of the $(A + k)$th alternative (numbering of the alternatives is identical to the ordering of the Alternative matrix) to be chosen for the jth variable; R_e is the effective radius in which accumulative fitness of the alternative A's neighbors are affected from its fitness. This radius is recommended to be not more than 1/4 of the search space; *Fitness* (i) is the fitness of location *i*.

It should be added that for alternatives close to edges (where $A + k$ is not a valid; $A + k < 0$ or $A + k > LA_j$), the *AF* is calculated using a reflective characteristic. In this case, if the distance of an alternative to the edge is less than R_e, it is assumed that the same alternative exists where picture of the mentioned alternative can be seen, if a mirror is placed on the edge.

(b) In order to distribute the possibility much evenly in the search space, a small value of ε is added to all the arrays as $AF = AF + \varepsilon$. Here, ε should be chosen according to the way the fitness is defined. It is better to be less than the minimum value achieved for the fitness.
(c) Find the best location of this loop and name it "The best location". Find the alternatives allocated to the variables of the best location, and let their *AF* be equal to zero.

In other words:

for j = 1: Number of variables
  for i = 1: Number of alternatives
    if i = The best location(j)

$$AF_{ij} = 0 \quad (3)$$

    end
  end
end

5. for variable $j_{(j=1toNV)}$, calculate the probability of choosing alternative $i_{(i=1toALj)}$, according to the following relationship:

Table 5
Optimal design comparison for the 25-bar spatial truss (Case 2).

Element group		Optimal cross-sectional areas (in^2)							
		Wu and Chow [22]	Li et al. [24]			Kaveh and Talatahar [25] HPSACO		Present study	
		GA	PSO	PSOPC	HPSO	$in.^2$	cm^2	$in.^3$	cm^3
1	A1	0.31	1.00	0.11	0.11	0.11	0.72	0.11	0.72
2	A_2–A_5	1.99	2.62	1.56	2.13	2.13	13.74	2.13	13.74
3	A_6–A_9	3.13	2.62	3.38	2.88	2.88	18.58	2.88	18.58
4	A_{10}–A_{11}	0.11	0.25	0.11	0.11	0.11	0.72	0.11	0.72
5	A_{12}–A_{13}	0.14	0.31	0.11	0.11	0.11	0.72	0.11	0.72
6	A_{14}–A_{17}	0.77	0.60	0.77	0.77	0.77	4.94	0.77	4.94
7	A_{18}–A_{21}	1.62	1.46	1.99	1.62	1.62	10.45	1.62	10.45
8	A_{22}–A_{25}	2.62	2.88	2.38	2.62	2.62	16.90	2.62	16.90
Weight (lb)		556.43	567.49	567.49	551.14	551.1	249.99	551.1	249.99

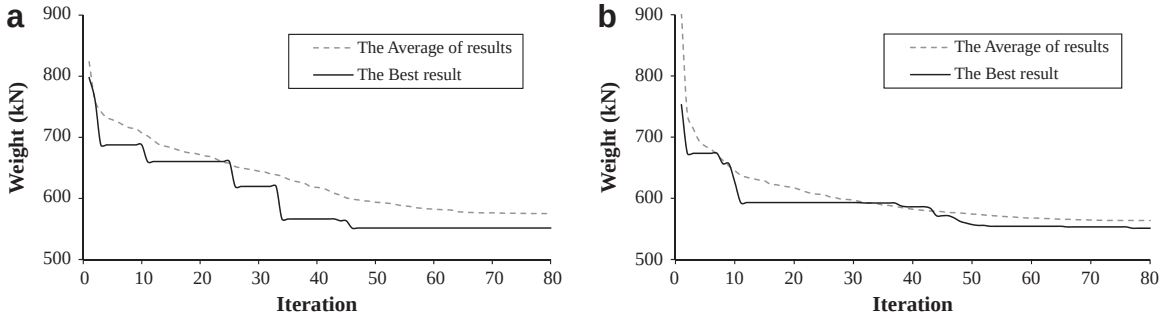

Fig. 12. The optimum answer convergence history for the 25-bar truss using DE. (a) Case 1, (b) Case 2.

$$P_{ij} = \frac{AF_{ij}}{\sum_{i=1}^{LAj} AF_{ij}} \tag{4}$$

6. Assign a probability equal to *PP* to all alternatives chosen for all variables of the best location and devote rest of the probability to the other alternatives according to the following formula:

for j = 1: Number of variables
  for i = 1: Number of alternatives
    if i = The best location(j)
      $P_{ij} = PP$ (5)
    else
      $P_{ij} = (1 - PP)P_{ij}$ (6)
    end
  end
end

Calculate the next step locations according to the probabilities assigned to each alternative.

Repeat Steps 2–6 as many times as the *Loops Number*.

3.3. Parameters of algorithm

Input parameters for the algorithm are:

(a) Loops number

For an optimization algorithm it is beneficial for the user to be able to dictate the algorithm to work according to the affordable computational cost. The answers may obviously be dependent on the selected number of loops and will improve by an increase in the loops number. However, the point is that one may not achieve results as bad as those of other optimization algorithms gained in less loops, because in this case although the algorithm quit its job much sooner than expected, the answer is good because of convergence criteria being reached. The number of loops can be selected by sensitivity analysis when high accuracy is required, however, in structural optimization of normal buildings, the loops number is recommended to be more than 50.

(b) Convergence curve formula

This is another important parameter to be selected for the algorithm. The curve should reach to the final point of 100% smoothly. If the curve satisfies the above mentioned criteria the algorithm will perform the job properly, but it is recommended to start with a linear curve and try the curves that spend more time (more loops) in high values of the *PP*. For example, if one is using proposed curves of this paper, it is recommended to start with *Power* = 1 which usually gives good results and it is better to try some cases of the *Power* < 1 to check if it improves the results.

(c) Effective radius (R_e)

This parameter is better to be chosen according to the size of search space. It is recommended to be selected less than 1/4 of the size of the search space.

(d) ε

This parameter is better to be less than any possible fitness.

(e) Number of locations (*NL*)

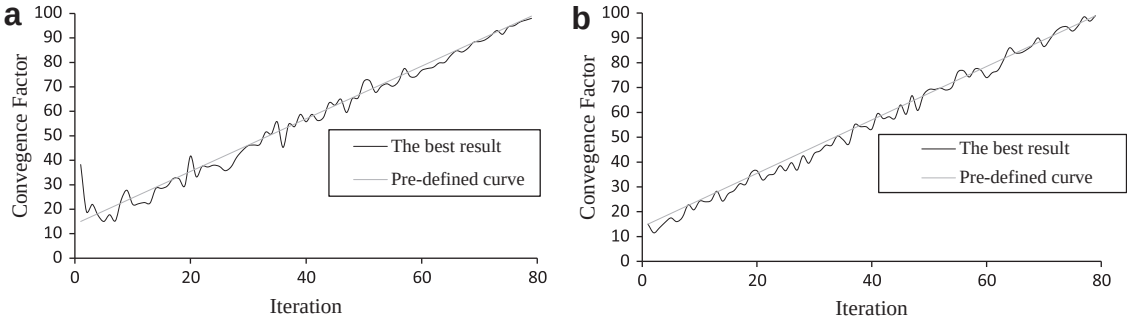

Fig. 13. The optimum answer and the average answers' convergence factor history for the 25-bar truss structure using the DE. (a) Case 1. (b) Case 2.

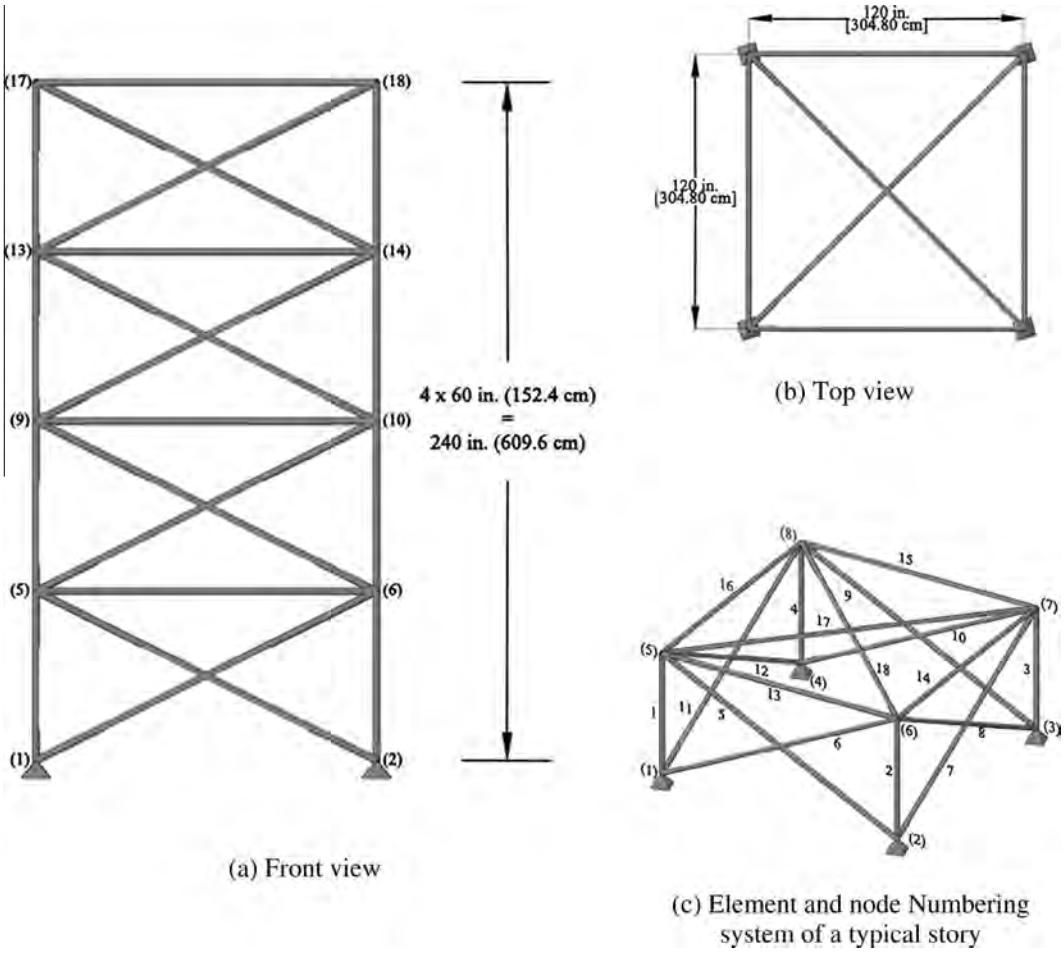

Fig. 14. A 72-bar spatial truss.

Table 6
Loading conditions for the 72-bar spatial truss.

Node	Case 1			Case 2		
	P_X kips (kN)	P_Y kips (kN)	P_Z kips (kN)	P_X kips (kN)	P_Y kips (kN)	P_Z kips (kN)
17	5.0 (22.25)	5.0 (22.25)	−5.0 (22.25)	0	0	−5.0 (22.25)
18	0.0	0.0	0.0	0.0	0.0	−5.0 (22.25)
19	0.0	0.0	0.0	0.0	0.0	−5.0 (22.25)
20	0.0	0.0	0.0	0.0	0.0	−5.0 (22.25)

Table 7
Optimal design comparison for the 72-bar spatial truss (Case 1).

Element group		Optimal cross-sectional areas (in.^{2})					
		Wu and Chow [22] GA	Lee and Geem [23] HS	Kaveh et al. [25] DHPSACO		Present work DE	
		in.^{2}	in.^{2}	in.^{2}	cm^2	in.^{2}	cm^2
1	A_1–A_4	1.5	1.9	1.9	12.26	2.0	12.90
2	A_5–A_{12}	0.7	0.5	0.5	3.23	0.5	3.23
3	A_{13}–A_{16}	0.1	0.1	0.1	0.65	0.1	0.65
4	A_{17}–A_{18}	0.1	0.1	0.1	0.65	0.1	0.65
5	A_{19}–A_{22}	1.3	1.4	1.3	8.39	1.3	8.39
6	A_{23}–A_{30}	0.5	0.6	0.5	3.23	0.5	3.23
7	A_{31}–A_{34}	0.2	0.1	0.1	0.65	0.1	0.65
8	A_{35}–A_{36}	0.1	0.1	0.1	0.65	0.1	0.65
9	A_{37}–A_{40}	0.5	0.6	0.6	3.87	0.5	3.23
10	A_{41}–A_{48}	0.5	0.5	0.5	3.23	0.5	3.23
11	A_{49}–A_{52}	0.1	0.1	0.1	0.65	0.1	0.65
12	A_{53}–A_{54}	0.2	0.1	0.1	0.65	0.1	0.65
13	A_{55}–A_{58}	0.2	0.2	0.2	1.29	0.2	1.29
14	A_{59}–A_{66}	0.5	0.5	0.6	3.87	0.6	3.87
15	A_{67}–A_{70}	0.5	0.4	0.4	2.58	0.4	2.58
16	A_{71}–A_{72}	0.7	0.6	0.6	3.87	0.6	3.87
Weight (lb)		400.66	387.94	385.54	174.9 kg	385.54	174.9 kg

Table 8
Optimal design comparison for the 72-bar spatial truss (Case 2).

Element group		Optimal cross-sectional areas (in.^{2})				
		Wu et al. [22] GA	Kaveh et al. [25] DHPSACO		Present work DE	
		in.^{2}	in.^{2}	cm^2	in.^{2}	cm^2
1	A_1–A_4	0.196	1.800	11.610	2.130	13.742
2	A_5–A_{12}	0.602	0.442	2.850	0.442	2.852
3	A_{13}–A_{16}	0.307	0.141	0.910	0.111	0.716
4	A_{17}–A_{18}	0.766	0.111	0.720	0.111	0.716
5	A_{19}–A_{22}	0.391	1.228	7.920	1.457	9.400
6	A_{23}–A_{30}	0.391	0.563	3.630	0.563	3.632
7	A_{31}–A_{34}	0.141	0.111	0.720	0.111	0.716
8	A_{35}–A_{36}	0.111	0.111	0.720	0.111	0.716
9	A_{37}–A_{40}	1.800	0.563	3.630	0.442	2.852
10	A_{41}–A_{48}	0.602	0.563	3.630	0.563	3.632
11	A_{49}–A_{52}	0.141	0.111	0.720	0.111	0.716
12	A_{53}–A_{54}	0.307	0.250	1.610	0.111	0.716
13	A_{55}–A_{58}	1.563	0.196	1.270	0.196	1.265
14	A_{59}–A_{66}	0.766	0.563	3.630	0.563	3.632
15	A_{67}–A_{70}	0.141	0.442	2.850	0.307	1.981
16	A71–A72	0.111	0.563	3.630	0.563	3.632
Weight (lb)		427.203	393.380	178.4 kg	391.329	177.47 kg

This parameter is the same as the population size in GA or number of ants in ACO. It should be chosen in a reasonable way.

3.4. Comprehensive numerical example

As an example consider the following simple mathematical function optimization problem:

$$\min\left(h=\sum_{i=1}^{N}x_i^2\right),\quad x_i\in Z,-20\leqslant x_i\leqslant 20 \tag{7}$$

Considering $N = 4$, dolphin echolocation algorithm suggests the following steps:

Before starting the optimization process for the changes of CF, a curve should be selected using Eq. (1), utilizing Power = 1, Loops number = 8, and $PP_1 = 0.1$, as follow:

$$PP=0.1+0.9\left(\frac{Loop_i-1}{7}\right)=0.1+0.9(Loop_i-1) \tag{8}$$

It should be noted that the PP_1 is better to be considered as the *CF* of the randomly selected generation of the first loop, which is equal to 0.11 for this example.

Dolphin echolocation steps to solve the problem are as follows:

1. Create the initial locations randomly, which includes the generating *NL* vectors consisting of *N* integer numbers between −20 and 20. For example, considering *NL* and *N* equal to 30 and 4, 30 vectors of length 4 should be selected randomly. One possible answer for the *i*th location can be $L_i = \{-10, 4, -7, 18\}$.
2. Calculate the *PP* of the loop using Eq. (8).
3. Calculate fitness for each location. In this example as the objective function is defined by Eq. (7), for the considered location (L_i), $h = (-10)^2 + 4^2 + (-7)^2 + 18^2 = 489$. As in DE, the fitness is

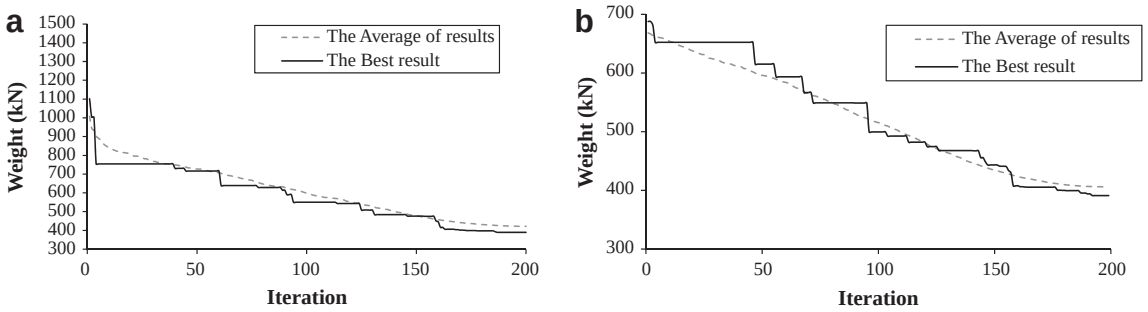

Fig. 15. The optimum answer and average answers' convergence history for the 72-bar truss using the DE. (a) Case 1, (b) Case 2.

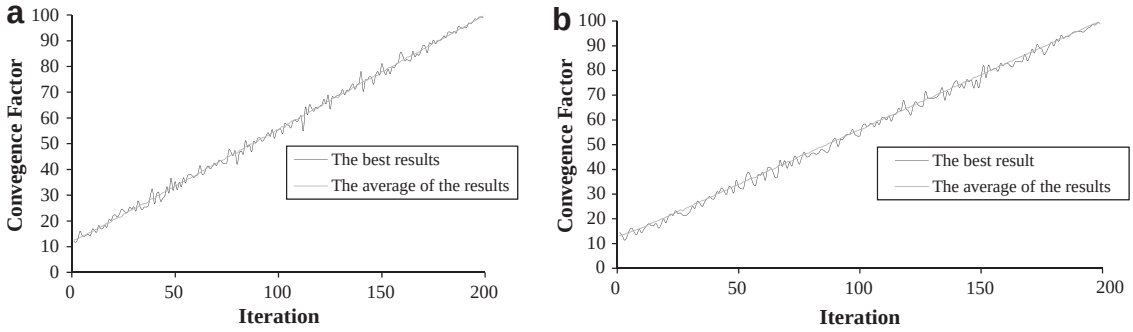

Fig. 16. The optimum answer and the average answers'convergence factor history for the 72-bar truss structure using the DE. (a) Case 1, (b) Case 2.

used to calculate the probability. Better fitnesses should have higher possibilities, then we can use $Fitness = 1/h$. It should be added that, for this special case, as h can be equal to zero, small value of 1 is added to the h in order to prevent the error of dividing by zero. Then the $Fitness = 1/(h+1)$, and for the considered location $Fitness(L_i) = 1/(489+1)=0.00204$.

4. Calculate the Accumulative fitness, using Eq. (2). As discussed before the alternatives should be sorted in an ascending order. The $Alternatives_{MA*NV}$ (MA is the number of alternatives, and NV is the number of optimization variables) is allocated to the possible alternatives for variables. For this example, the Alternatives matrix is:

$$Alternatives = \begin{bmatrix} -20 & -20 & -20 & -20 \\ -19 & -19 & -19 & -19 \\ . & . & . & . \\ . & . & . & . \\ . & . & . & . \\ 19 & 19 & 19 & 19 \\ 20 & 20 & 20 & 20 \end{bmatrix} \quad (9)$$

Then for sample location, L_i, considering $R_e = 10$, Eq. (2) becomes:

```
for i = L_i
  for j = 1 to 4
    find the position of L(i,j) in the jth column of the
   Alternatives matrix and name it as A.
    for k = −10 to 10
      AF_(A+k)j = 1/10 * (10 − |k|)Fitness(L_i) + AF_(A+k)j        (10)
    end
  end
end
```

Eq. (10) can also be stated as:

```
for j = {1,2,3,4}
  L(i,j) = {−10,4,−7,18}, then A = {11,25,14,39}
  for k = −10 to 10
    AF_(11+k)1 = 1/10 * (10 − |k|)Fitness(L_i) + AF_(11+k)1      (11)
    AF_(25+k)2 = 1/10 * (10 − |k|)Fitness(L_i) + AF_(25+k)2
    AF_(14+k)3 = 1/10 * (10 − |k|)Fitness(L_i) + AF_(14+k)3
    AF_(39+k)4 = 1/10 * (10 − |k|)Fitness(L_i) + AF_(39+k)4
  end
end
```

Considering ε as the worth possible fitness, it will be $\varepsilon = 1/(4 * 20^2)$ and then $AF = AF + 0.000625$.

In these equations, it can be seen that for example for $j = 2$ (the second variable), for calculating the accumulative fitness, search space should be divided into two regions: affected region (in effective radius) and not affected region. Choosing R_e equal to 10, alternatives with absolute distance to 4 (alternative 4 is chosen for the second variable) more than 10 ($x < -6$ and $x > 14$) are considered not affected. Also in the affected area the accumulative fitness resulted from this sample location changes linearly in a way that its maximum appears in $x = 4$. The accumulative fitness to be added for this alternative is:

$$AF_{(x+25)2} = AF_{(x+25)2} + \begin{cases} 0 & x < -6 \\ \frac{Fitness(Li)}{10}(x+6) & -6 < x \leqslant 4 \\ \frac{Fitness(Li)}{10}(14-x) & 4 < x \leqslant 14 \\ 0 & x > 14 \end{cases} \quad (12)$$

$$AF = AF + 0.000625$$

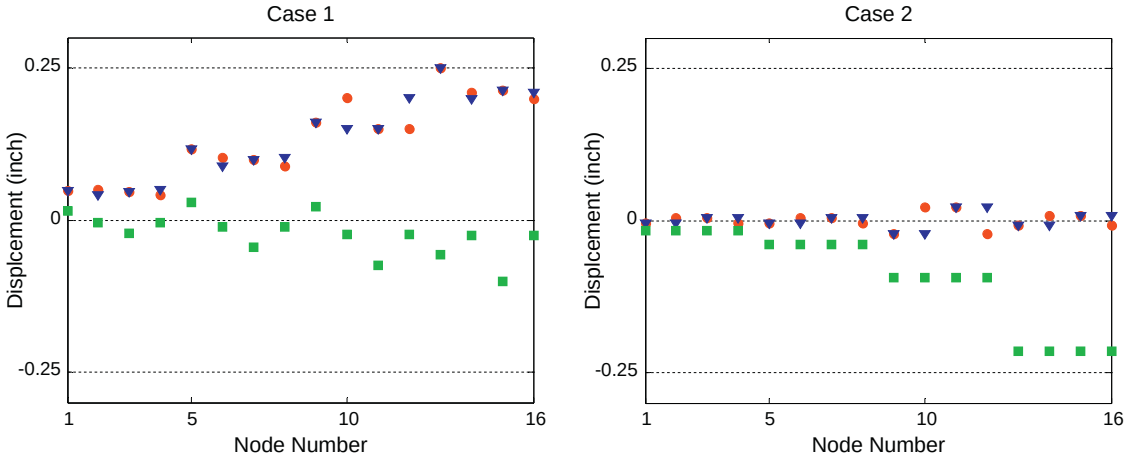

Fig. 17. Comparison of the allowable and existing displacements for the nodes of the 72-bar truss structure using the DE.

Fig. 4 shows the result of performing the explained process for all four variables of this location.

Performing Step 4 for all the randomly selected answers, the final Accumulative fitness of the first loop is achieved.

5. For variable $j_{(j=1\text{to}4)}$, calculate the probability of choosing alternative $i_{(i=1\text{to}40)}$, according to the following relationship:

$$P_{ij} = \frac{AF_{ij}}{\sum_{k=1}^{40} AF_{kj}} \tag{13}$$

and consequently the probability will be according to Figs. 5 and 6.

6. Fig. 5 demonstrates the accumulative fitness of variables $X1$, $X2$, $X3$ and $X4$. The best location of the first loop is achieved by setting variables as: $X1 = -11$, $X2 = 3$, $X3 = X4 = 4$. On the other hand, according to Eq. (8), PP for the first loop is equal to 10%, as a result all variables in their best placement is equal to 10% probability of the other alternatives is defined distributing remaining value of probability equal to 90% to the other alternatives, using the following formula:

$$P_{ij} = (1 - 0.1)P_{ij} = 0.9P_{ij} \tag{14}$$

Since the number of loops is equal to 8, Steps 2–6 should be repeated 8 times.

Figs. 7–10 show the accumulative fitness and the probability of alternatives in loops 4 and 8, respectively. It can be seen from these figures that the probability changes in a way that in 8 loops DE reaches the best answer.

3.5. Comparison between the dolphin echolocation and bat inspired algorithm

Bat inspired algorithm can be considered as a balanced combination of the standard particle swarm optimization and the intensive local search controlled by the loudness and pulse rate [17]. In this algorithm loudness and pulse frequency are echolocation parameters that gradually restrict the search according to pulse emission and loudness rules. This is while, in dolphin echolocation algorithm there is no movement to the best answer. DE algorithm works with possibilities.

4. Structural optimization

In this study the structural optimization goal is to minimize the weight of the structure that is formulated as follows:

$$\text{Minimize}: \quad w = \rho \sum_{i=1}^{M} A_i L_i \tag{15}$$

$$\text{s.t.}: \quad KU - P = 0 g_1 \geqslant 0, \quad g_2 \geqslant 0, \ldots, g_n \geqslant 0 \tag{16}$$

where $g_1, g_2, \ldots, g_n$ are constraint functions depending on the element being used in each problem and K, U and P are the stiffness matrix, nodal displacement and nodal force vectors, respectively. In this study, different constraints are implemented for structural design including drift, displacement and strength. Constraints are clarified in numerical examples.

Furthermore, such a constrained formulation is treated in an unconstrained form, using a penalized fitness function as:

$$F = F_0 - w * (1 + K_p \cdot V) \tag{17}$$

where F_0 is a constant taken as zero for the class of considered examples. K_p is the penalty coefficient, and V denotes the total constraints' violation considering all the load combinations.

5. Numerical examples

In this section three trusses and two frames are optimized using the present algorithm and the results are compared to those of some other existing approaches. The algorithms are coded in Matlab and structures are analyzed using the direct stiffness method.

5.1. Truss structures

In the following three trusses are optimized and the results of the present algorithm are compared to those of different algorithm.

5.1.1. A 25-bar spatial truss

The 25-bar spatial truss structure shown in Fig. 11 has been studied in [22–24]. The material density is 0.1 lb/in.^{3} (2767.990 kg/m^3) and the modulus of elasticity is 10,000 ksi (68,950 MPa). The stress limitations of the members are ±40 kpsi (±275.80 MPa). All nodes in three directions are subjected to displacement limitations of ±0.35 inch (in.) (±8.89 mm) imposed on every node in each direction. The structure includes 25 members, which are divided into eight groups, as follows: (1) A_1, (2) A_2–A_5, (3) A_6–A_9, (4) A_{10}–A_{11}, (5) A_{12}–A_{13}, (6) A_{14}–A_{17}, (7) A_{18}–A_{21} and (8) A_{22}–A_{25}. Two optimization cases are implemented.

Case 1: The discrete variables are selected from the set $D = \{0.01, 0.4, 0.8, 1.2, 1.6, 2.0, 2.4, 2.8, 3.2, 3.6, 4.0, 4.4, 4.8, 5.2, 5.6, 6.0\}$ (in.^{2}) or $\{0.065, 2.58, 5.16, 7.74, 10.32, 12.90, 15.48, 18.06, 20.65, 23.22, 25.81, 28.39, 30.97, 33.55, 36.13, 38.71\}$ (cm^2).

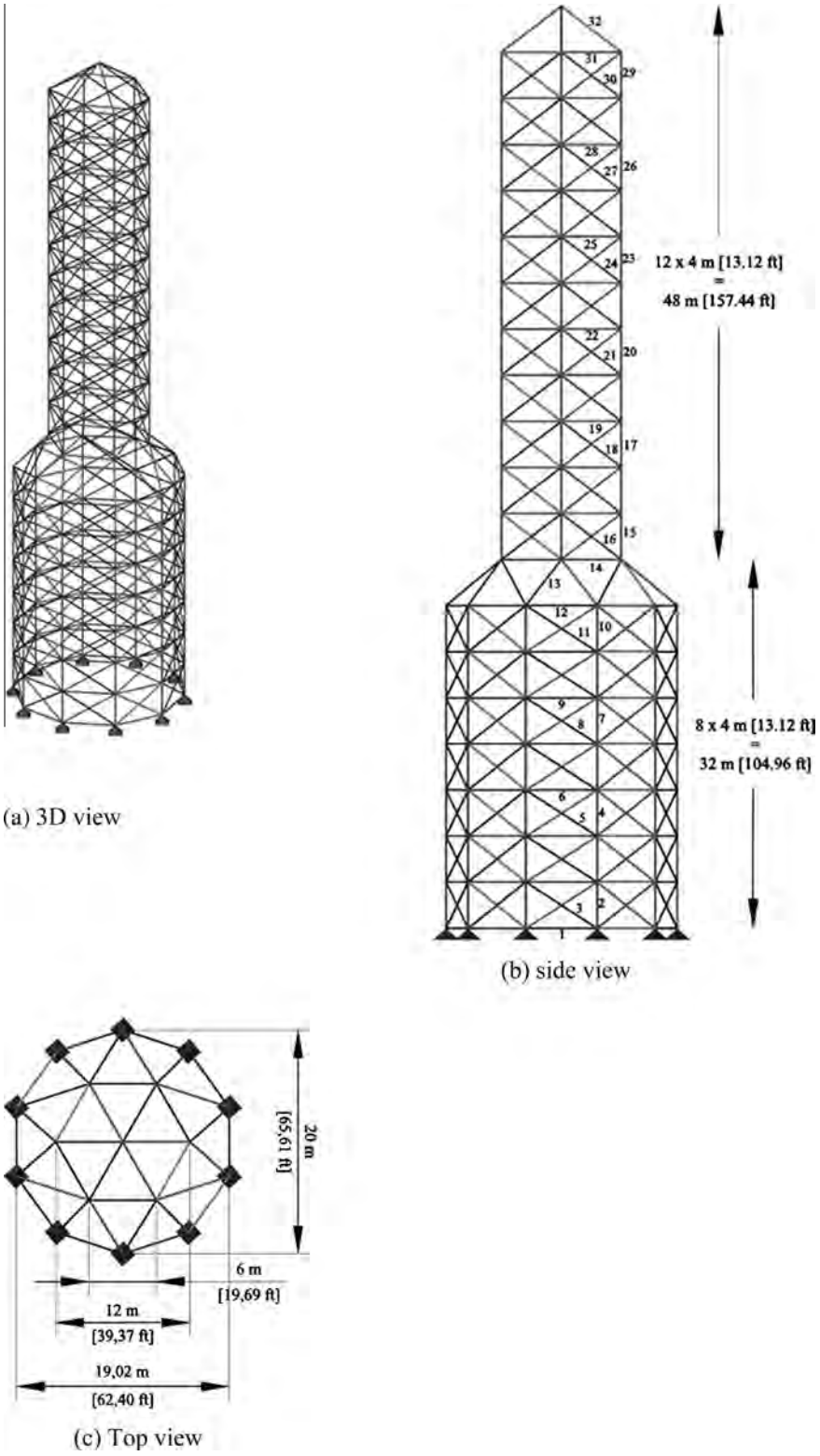

Fig. 18. A 582-bar tower truss.

Case 2: The discrete variables are selected from the [26], listed in Table 2. The loads for both cases are shown in Table 3.

For solving this problem by the use of DE, Loops number is set to 80. Convergence curve is according to Eq. (1) considering $PP_1 = 0.15$ and *Power* = 0.2. R_e and ε are equal to 5 and 1, respectively.

According to Tables 4 and 5 and Fig. 12, DE achieves the best answer in approximately 50 loops in Case 1 and near 80 loops in Case 2, while HPSACO reaches to the same result in around 100 loops. It should be mentioned that Kaveh and Talatahari [12] show that the HPSACO itself has better convergence rate in comparison to GA, PSO, PSOPC and HPSO.

Table 9
Optimal design comparison for the 582-bar spatial truss.

Element group	Optimal cross-section					
	Case 1				Case 2	
	Hasançebi et al. [27] (PSO) Ready section	Sonmez [30] (ABC) Ready section	Kaveh et al. [29] (DHPSACO) Ready section	Present work (DE) Ready section	Sonmez [30] (ABC) Ready section	Present work (DE) Ready section
1	W8X21	W8X22	W8X24	W8X21	W8X22	W8X21
2	W12X79	W12X97	W12X72	W12X96	W10X78	W27X94
3	W8X24	W8X25	W8X28	W8X24	W8X25	W8X24
4	W10X60	W12X59	W12X58	W12X58	W14X62	W12X58
5	W8X24	W8X24	W8X24	W8X24	W8X24	W8X24
6	W8X21	W8X21	W8X24	W8X21	W8X21	W8X21
7	W14X48	W12X46	W10X49	W12X45	W12X51	W12X50
8	W8X24	W8X24	W8X24	W8X24	W8X24	W8X24
9	W8X21	W8X21	W8X24	W8X21	W8X21	W8X21
10	W10X45	W12X46	W12X40	W12X45	W10X50	W12X45
11	W8X24	W8X22	W12X30	W8X21	W8X25	W8X21
12	W10X68	W12X66	W12X72	W12X65	W10X69	W12X72
13	W14X74	W10X77	W18X76	W10X77	W18X77	W14X74
14	W14X48	W10X49	W10X49	W10X49	W14X49	W12X50
15	W18X76	W14X83	W14X82	W14X82	W10X78	W10X68
16	W8X31	W8X32	W8X31	W8X31	W8X32	W8X31
17	W16X67	W12X53	W14X61	W10X60	W21X62	W14X61
18	W8X24	W8X24	W8X24	W8X24	W8X24	W8X24
19	W8X21	W8X21	W8X21	W8X21	W8X21	W8X21
20	W8X40	W16X36	W12X40	W12X45	W14X43	W14X43
21	W8X24	W8X24	W8X24	W8X21	W8X24	W8X21
22	W8X21	W10X22	W14X22	W8X21	W8X21	W8X21
23	W10X22	W10X22	W8X31	W10X22	W8X24	W6X25
24	W8X24	W6X25	W8X28	W8X21	W8X24	W8X21
25	W8X21	W8X21	W8X21	W8X21	W8X21	W8X21
26	W8X21	W8X21	W8X21	W8X21	W8X21	W8X21
27	W8X24	W8X24	W8X24	W8X21	W8X24	W8X21
28	W8X21	W8X21	W8X28	W8X21	W8X21	W8X21
29	W8X24	W8X22	W16X36	W8X21	W8X21	W8X21
30	W8X21	W10X23	W8X24	W8X21	W8X21	W8X21
31	W8X21	W8X25	W8X21	W8X21	W8X24	W8X21
32	W8X24	W6X26	W8X24	W8X21	W8X24	W8X21
Best (lb)	363795.7	368484.1	380982.7	360367.8	365906.3	360143.3
Average (lb)	365124.9	370178.6	–	364404.7	366088.4	362207.1
Worst (lb)	370159.1	373530.3	–	371922.1	369162.2	367512.2
Evaluations(#)	50,000	50,000	8500	25,000	100,000	50,000
Differences compared to DE	0.95%	2.25%	5.72%		1.60%	

In addition, Fig. 13 shows the convergence factor history. It can be seen that the algorithm follows the predefined linear curve as expected.

5.1.2. A 72-bar spatial truss

For the 72-bar spatial truss structure shown in Fig. 14, the material density is 0.1 lb/in.^{3} (2767:990 kg/m^3) and the modulus of elasticity is 10,000 ksi (68,950 MPa). The members are subjected to the stress limits of ±25 ksi (±172.375 MPa). The nodes are subjected to the displacement limits of ±0.25 in. (±0.635 cm).

The 72 structural members of this spatial truss are sorted into 16 groups using symmetry: (1) A_1–A_4, (2) A_5–A_{12}, (3) A_{13}–A_{16}, (4) A_{17}–A_{18}, (5) A_{19}–A_{22}, (6) A_{23}–A_{30}, (7) A_{31}–A_{34}, (8) A_{35}–A_{36}, (9) A_{37}–A_{40}, (10) A_{41}–A_{48}, (11) A_{49}–A_{52}, (12) A_{53}–A_{54}, (13) A_{55}–A_{58}, (14) A_{59}–A_{66} (15), A_{67}–A_{70}, and (16) A_{71}–A_{72}.

Two optimization cases are implemented.

Case 1: The discrete variables are selected from the set $D = \{0.1, 0.2, 0.3, 0.4, 0.5, 0.6, 0.7, 0.8, 0.9, 1.0, 1.1, 1.2, 1.3, 1.4, 1.5, 1.6, 1.7, 1.8, 1.9, 2.0, 2.1, 2.2, 2.3, 2.4, 2.5, 2.6, 2.7, 2.8, 2.9, 3.0, 3.1, 3.2\}$ (in.^{2}) or $\{0.65, 1.29, 1.94, 2.58, 3.23, 3.87, 4.52, 5.16, 5.81, 6.45, 7.10, 7.74, 8.39, 9.03, 9.68, 10.32, 10.97, 12.26, 12.90, 13.55, 14.19, 14.84, 15.48, 16.13, 16.77, 17.42, 18.06, 18.71, 19.36, 20.00, 20.65\}$ (cm^2).

Case 2: The discrete variables are selected from Table 2.

Table 6 lists the values and directions of the two load cases applied to the 72-bar spatial truss.

The problem has been solved by GA [22,23] and DHPSO [25].

Solving the problem using DE, the Loops number is set to 200. Convergence curve is according to Eq. (1) considering $PP_1 = 0.15$ and $Power = 1$. R_e and ε are equal to 5 and 1, respectively.

It can be seen from Table 7 that in Case 1 the best answer is achieved using DE that is better than GA and HS and although it is the same as DHPACO, but the penalty of the optimum answer is less than that of the DHPACO. Moreover Table 8 shows that in Case 2, the DE achieves better results in comparison to the previously published works. Fig. 15 shows that the DE can converge to the best answer in 200 loops, then it has higher convergence rate compared to the other algorithms.

In addition, Fig. 16 shows the convergence factor history. It can be seen that the algorithm follows the predefined linear curve as expected.

Fig. 17 shows the allowable and existing displacements for the nodes of the 72-bar truss structure using the DE.

5.1.3. A 582-bar tower truss

The 582-bar tower truss shown in Fig. 18, is chosen from Ref. [27]. The symmetry of the tower about *x*-axis and *y*-axis is consid-

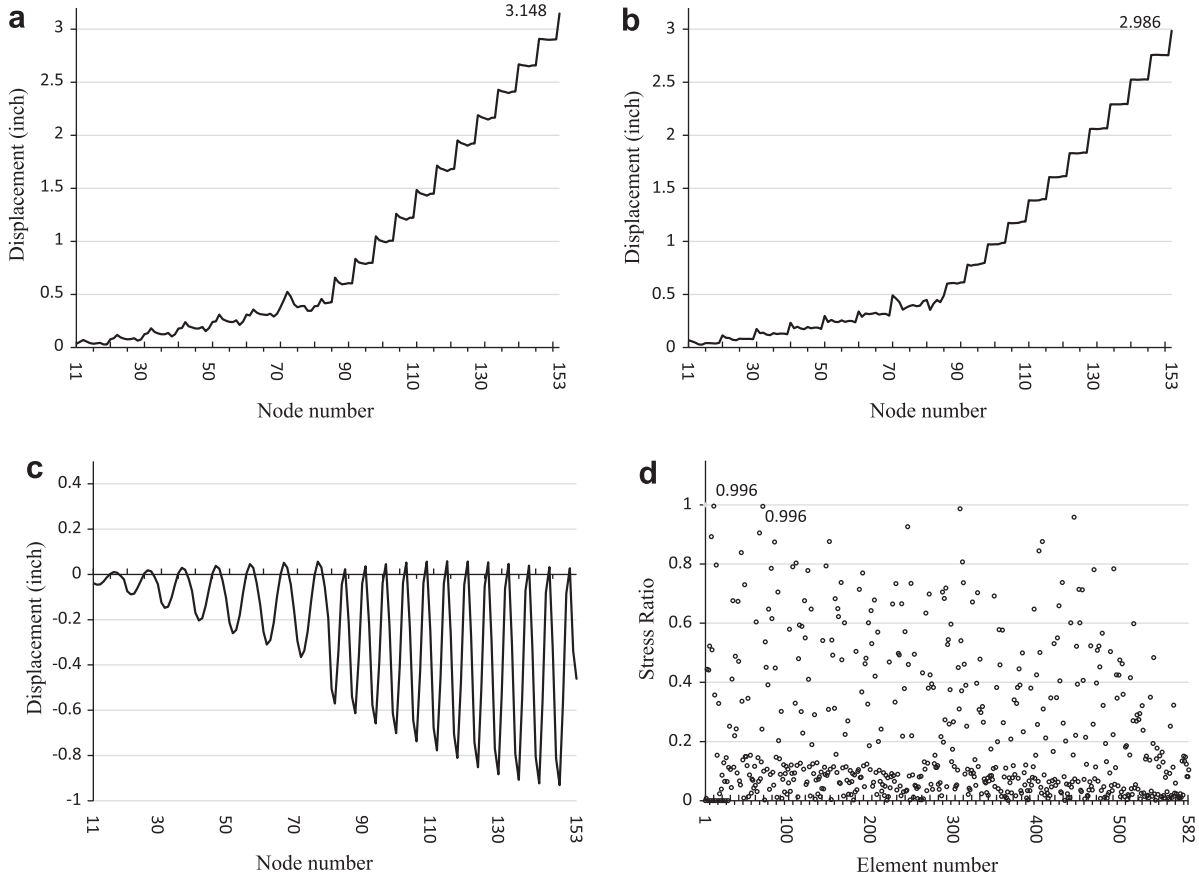

Fig. 19. Comparison of the allowable and existing constrains for the 582-bar truss, Case 2 using DE. (a) Displacement in the *x*-direction, (b) displacement in *y*-direction, (c) displacement in the *z*-direction, (d) stress ratios.

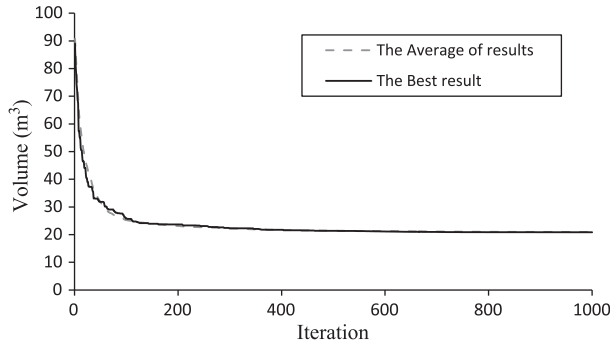

Fig. 20. Convergence history of optimum result and average results for the 582-bar tower truss, Case 2, using DE.

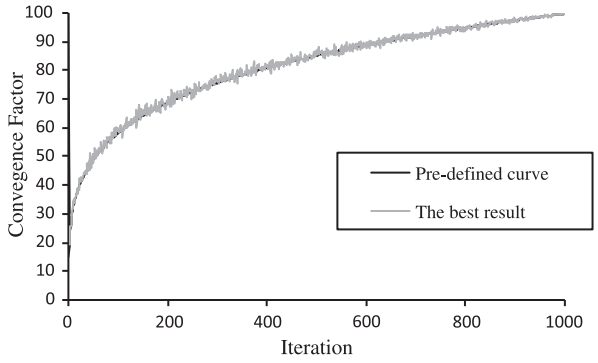

Fig. 21. The convergence factor history for the 582-bar tower truss, Case 2 using DE.

ered to group the 582 members into 32 independent size variables. A single load case is considered consisting of the lateral loads of 5.0 kN (1.12 kips) applied in both *x*- and *y*-directions and a vertical load of 30 kN (6.74 kips) applied in the *z*-direction at all nodes of the tower. A discrete set of 140 economical standard steel sections selected from W-shape profile list based on area and radii of gyration properties is used to size the variables, [27]. The lower and upper bounds on size variables are taken as 6.16 in.^{2} (39.74 cm^2) and 215.0 in.^{2} (1387.09 cm^2), respectively. The stress limitations of the members are imposed according to the provisions of ASD-AISC [26] as follows:

$$\begin{cases} \sigma_i^+ = 0.6Fy & \text{for } \sigma_i \geqslant 0 \\ \sigma_i^- & \text{for } \sigma_i < 0 \end{cases} \tag{18}$$

where σ_i^- is calculated according to the slenderness ratio

$$\sigma_i^- = \begin{cases} \left[\left(1 - \frac{\lambda_i^2}{2C_i^2}\right)F_y\right] \Big/ \left(\frac{5}{3} + \frac{3\lambda_i}{8C_C} - \frac{\lambda_i^3}{8C_C^3}\right) & \text{for } \lambda_i < C_C \\ \frac{12\pi^2 E}{23\lambda_i^2} & \text{for } \lambda_i \geqslant C_C \end{cases} \tag{19}$$

where E = the modulus of elasticity; F_y = the yield stress of A36 steel; $C_C = \sqrt{2\pi^2 E/F_y}$; λ_i = the slenderness ratio (kL_i/r_i); k = the effective length factor; L_i = the member length; and r_i = the radius of gyration. The other constraint is the limitation of the nodal displacements (no more than 8.0 cm or 3.15 in for each direction). In

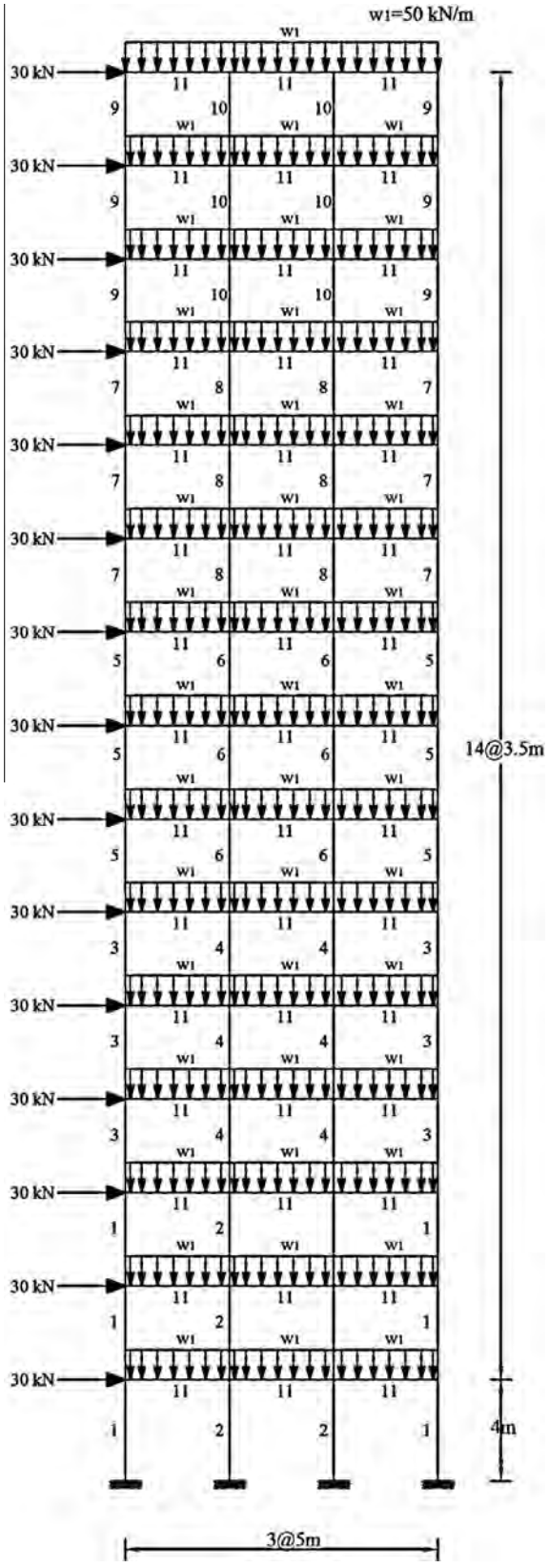

Fig. 22. Topology of the 3-bay 15-story planar frame.

addition, the maximum slenderness ratio is limited to 300 for the tension members, and this limit is recommended to be 200 for the compression members according to the ASD-AISC [26] design code provisions.

The problem was solved later by Kaveh and Talatahari [29] and Sonmez [30]. Two cases for analyzing are used according to Ref. [30], as follows:

Case 1: All members are selected from a set of 140W-shaped profiles according to Ref. [27] and the maximum number of evaluations is set to 50,000. For the DE, 25,000 evaluations are considered for this case to demonstrate the efficiency of the algorithm.
Case 2: There is no difference between Case 1 and Case 2, but in the number of evaluations which is set to 100,000. For the DE, 50,000 evaluations are considered for this case to demonstrate efficiency of the algorithm.

Convergence curve is according to Eq. (1) considering $PP_1 = 15\%$ and $Power = 0.2$. R_e and ε are equal to 10 and 1, respectively.

Results can be seen in Table 9, which shows that in Case 1, the DE outperforms the HPSACO, ABC and PSO by 5.7%, 2.3% and 1%, respectively, and in Case 2, the DE results is 1.6% better than those of ABC algorithm. In addition comparing the results with those presented in [27], it can be seen that the optimum answer of the DE in Case 1 is 1.1%, 1.3%, 2.2%, 2.7%, 4.7% and 6.7% lighter than those of the ESs, SA, TS, ACO, HS and SGA.

Fig. 19 shows the comparison of the allowable and existing constrains for the 582-bar truss using the DE. The maximum values for displacement in x, y and z directions are 3.148 in (7.995 cm), 2.986 in (7.584 cm) and 0.931 in (2.365 cm), respectively. The maximum stress ratio is 96.60%. It can be seen that some displacements and stresses are near the boundary conditions. It should be mentioned that there is a small difference between analysis results of Sap2000 (Hasançebi et al. [27]), C# programming language code (Sonmez [30]) and Matlab code (present study). Then checking the results of each code with another one may show a violation of constraints. Fig. 19 shows according to the finite element program coded in Matlab, there is no penalty for the best answer.

Fig. 20 shows the convergence history of the best answer and average results for the DE, and Fig. 21 illustrates the convergence factor history. It can be seen that the algorithm follows the predefined linear curve as expected.

5.2. Frame structures

The displacement and AISC combined strength constraints are the performance constraints of the frame as follows:

(a) Maximum lateral displacement:

$$\frac{\Delta_T}{H} < R \tag{20}$$

where Δ_T is the maximum lateral displacement of the structure (the roof lateral displacement), H is the height of the structure, and R is the maximum drift index.

(b) The inter-story displacements:

$$\frac{d_j}{h_j} < R_I, \quad j = 1, 2, \ldots, ns \tag{21}$$

d_j is the inter-story drift which is used to give the relative displacement of each roof in comparison to its following floor; h_j is the story height of jth floor; ns is the total number of stories; R_I is the inter-story drift index which is equal to 1/300 according to the ANSI/AISC 360-05 (2005), Ref. [28].

Table 10
Optimal design comparison for the 3-bay 15-story planar frame.

Element group	Optimal W-shaped sections Kaveh and Talatahari					Present work
	PSO [29]	PSOPC [29]	HPSACO [29]	ICA [31]	CSS [14]	
1	W33X118	W27X129	W21X111	W24X117	W21X147	W12X87
2	W33X263	W24X131	W18X158	W21X147	W18X143	W36X182
3	W24X76	W24X103	W10X88	W27X84	W12X87	W21X93
4	W36X256	W33X141	W30X116	W27X114	W30X108	W18X106
5	W21X73	W24X104	W21X83	W14X74	W18X76	W18X65
6	W18X86	W10X88	W24X103	W18X86	W24X103	W14X90
7	W18X65	W14X74	W21X55	W12X96	W21X68	W10X45
8	W21X68	W27X94	W27X114	W24X68	W14X61	W12X65
9	W18X60	W21X57	W10X33	W10X39	W18X35	W6X25
10	W18X65	W18X71	W18X46	W12X40	W10X33	W10X45
11	W21X44	W21X44	W21X44	W21X44	W21X44	W21X44
Weight (kN)	496.68	452.34	426.36	417.466	412.62	395.35
Differences compared to DE	**26%**	**14%**	**8%**	**6%**	**4%**	

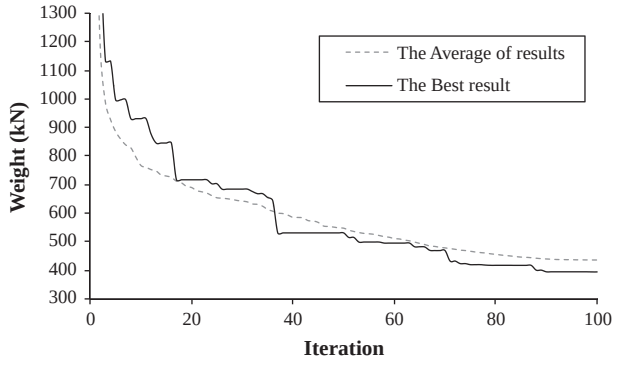

Fig. 23. The optimum answer and average answer with the convergence history for the 3-bay 15-story frame using the DE.

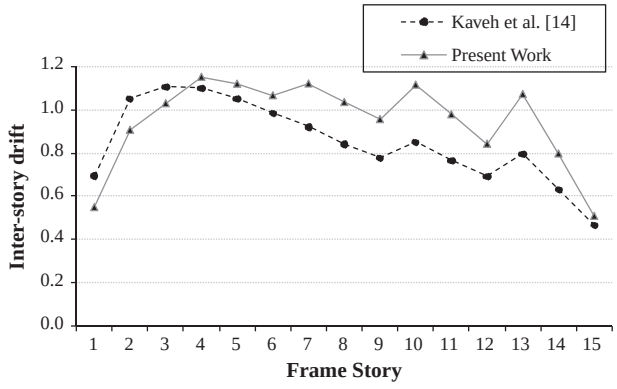

Fig. 24. Comparison of the allowable and the existing inter-story drift for the 3-bay 15-story planar frame.

(c) Element forces:

$$\frac{P_u}{2\phi_C P_n}+\frac{M_u}{\phi_b M_n}<1 \quad \text{for } \frac{P_u}{\phi_C P_n}<0.2$$
$$\frac{P_u}{\phi_C P_n}+\frac{8}{9}\frac{M_u}{\phi_b M_n}<1 \quad \text{for } \frac{P_u}{\phi_C P_n}\geqslant 0.2 \tag{22}$$

where P_u is the required strength (tension or compression); P_n is the nominal axial strength (tension or compression); ϕ_c is the axial resistance factor ($\phi_c = 0.9$ for tension, $\phi_c = 0.85$ for compression); M_u is required flexural strength; M_n is nominal flexural strength; and ϕ_b is the flexural resistance factor ($\phi_b = 0.9$)

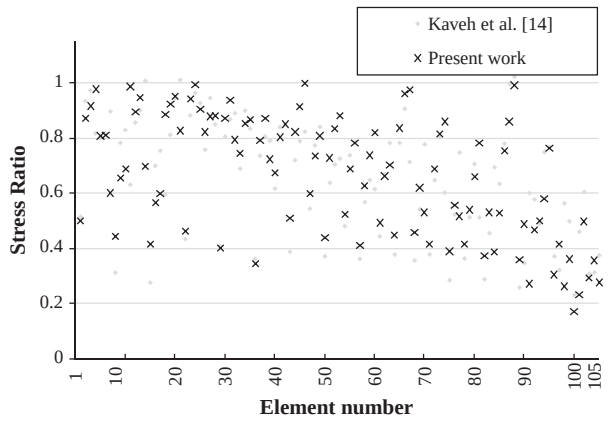

Fig. 25. Comparison of the allowable and the existing stress ratios for the 3-bay 15-story planar frame.

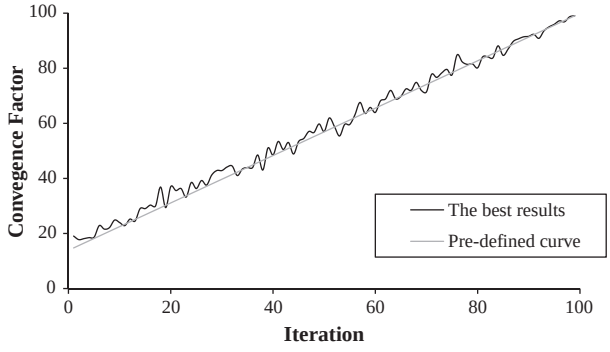

Fig. 26. The optimum answer and the average answer with the convergence factor history for the 3-bay 15-story planar frame using the DE.

5.2.1. A 3-bay 15-story planar frame

Fig. 22 shows the configuration and applied loads of a 3-bay 15-story frame structure choosen from Ref. [29]. This frame consists of 64 joints and 105 members. The sway of the top story is limited to 23.5 cm. The material has a modulus of elasticity equal to $E = 205$ GPa and a yield stress of $F_y = 248.2$ MPa. The effective length factors of the members are calculated as $K_x \geqslant 0$ for a sway-permitted frame and the out-of-plane effective length factor is specified as $K_y = 1.0$. Each column is considered as non-braced

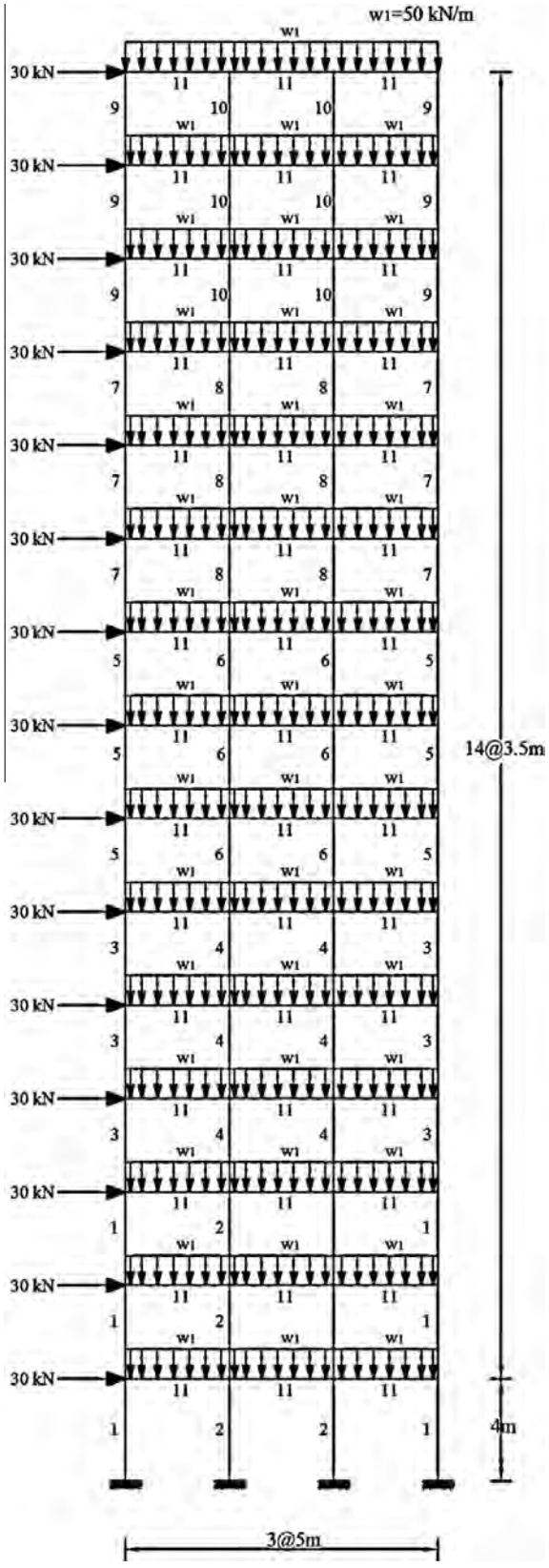

Fig. 27. Topology of the 3-bay 24-story planar frame.

along its length, and the unbraced length for each beam member is specified as one-fifth of the span length.

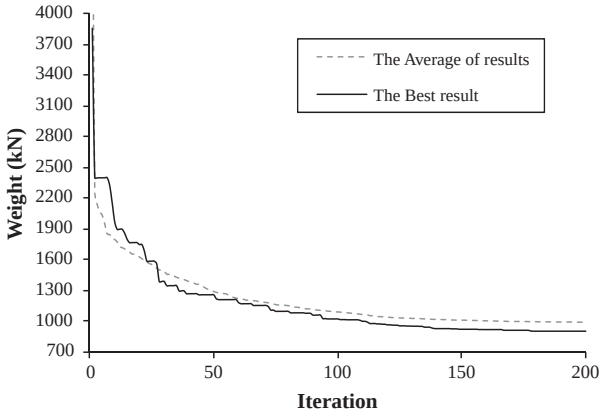

Fig. 28. The optimum answer and the average answer, with the convergence history for the 3-bay 24-story frame using the DE.

For solving this problem by DE, the Loops number is set to 100. The convergence curve is according to Eq. (1) considering $PP_1 = 0.15$ and *Power* = 1. R_e and ε are equal to 5 and 1, respectively.

Results of the present study and those of Refs. [14,29,31] are provided in Table 10. It can be seen that the DE achieves results that are 26%, 14%, 8%, 6% and 4% lighter than the PSO, PSOPC, HPSACO, ICA and CSS, respectively.

Convergence history is depicted in Fig. 23. It can be seen that the present algorithm leads to the best answer in 100 loops which is less than that of the CSS (250 loops).

The maximum value of displacement is 14.27 cm which is less than the allowable limit (23.5 cm).

Fig. 24 shows the inter-story drifts, the maximum value of which is 1.15 cm. This is less than the allowable value (1.17 cm). It can be recognized that by reducing the weight of structure its stiffness is reduced, then the inter-story drifts are closer to the maximum allowable value.

In Fig. 25 the stress ratios of the elements are shown. The maximum stress ratio is 99.69%. One can see that similar to the inter-story limitation, stress ratios are closer to the limit line.

Fig. 26 shows the *CF* changes during optimization. It is clear that the *CF* changes around predefined line.

5.2.2. A 3-bay 24-story planar frame

Fig. 27 shows the topology and the service loading conditions for a 3-bay 24-story frame consisting of 100 joints and 168 members which is chosen from Camp et al. [32]. The frame is designed following the LRFD specification and uses an inter-story drift displacement constraint. The material properties are a modulus of elasticity equal to $E = 205$ GPa and a yield stress of $F_y = 230.3$ MPa.

The effective length factors of the members are calculated as $K_x \geqslant 0$ for the sway-permitted frame and the out-of-plane effective length factor is specified as $K_y = 1.0$. All columns and beams are considered non-braced along their lengths. Fabrication conditions are imposed on the construction of the 168-element frame requiring that the same beam section be used in the first and third bay on all the floors except the roof beams, resulting in four beam groups.

Beginning at the foundation, the exterior columns are combined into one group and the interior columns are combined together in another group over three consecutive stories. The grouping results in 16 column sections and 4 beam sections for a total of 20 design variables. In this example, each of the four beam element groups is chosen from all 267W-shapes, while the 16 column element groups are limited to W14 sections (37W-shapes).

For solving this problem by the DE, the Loops number is set to be equal to 200. The convergence curve is according to Eq. (1) con-

Table 11
Optimal design comparison for the 3-bay 24-story planar frame.

Element group	Optimal W-shaped sections					Present work
	Camp et al. [32]	Degertekin [33]	Kaveh and Talatahari			
	ACO	HS	IACO [34]	ICA [31]	CSS[14]	
1	W30X90	W30X90	W30X99	W30X90	W30X90	W30X90
2	W8X18	W10X22	W16X26	W21X50	W21X50	W6X20
3	W24X55	W18X40	W18X35	W24X55	W21X48	W21X44
4	W8X21	W12X16	W14X22	W8X28	W12X19	W6X9
5	W14X145	W14X176	W14X145	W14X109	W14X176	W14X159
6	W14X132	W14X176	W14X132	W14X159	W14X145	W14X145
7	W14X132	W14X132	W14X120	W14X120	W14X109	W14X132
8	W14X132	W14X109	W14X109	W14X90	W14X90	W14X99
9	W14X68	W14X82	W14X48	W14X74	W14X74	W14X68
10	W14X53	W14X74	W14X48	W14X68	W14X61	W14X61
11	W14X43	W14X34	W14X34	W14X30	W14X34	W14X43
12	W14X43	W14X22	W14X30	W14X38	W14X34	W14X22
13	W14X145	W14X145	W14X159	W14X159	W14X145	W14X109
14	W14X145	W14X132	W14X120	W14X132	W14X132	W14X109
15	W14X120	W14X109	W14X109	W14X99	W14X109	W14X90
16	W14X90	W14X82	W14X99	W14X82	W14X82	W14X82
17	W14X90	W14X61	W14X82	W14X68	W14X68	W14X74
18	W14X61	W14X48	W14X53	W14X48	W14X43	W14X43
19	W14X30	W14X30	W14X38	W14X34	W14X34	W14X30
20	W14X26	W14X22	W14X26	W14X22	W14X22	W14X26
Weight (kN)	980.63	956.13	967.33	946.25	945.02	912.26
Difference compared to DE	**7.5%**	**4.8%**	**6.0%**	**3.7%**	**3.6%**	

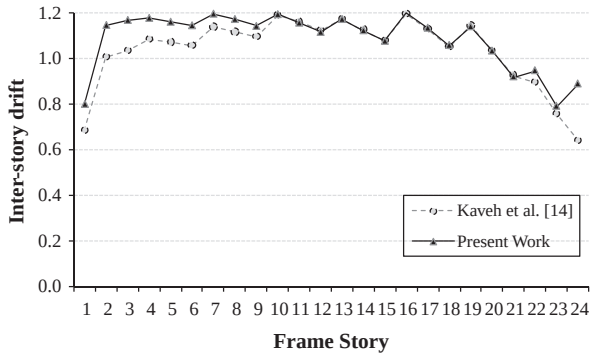

Fig. 29. Comparison of the allowable and the existing inter-story drift for the 3-bay 24-story planar frame.

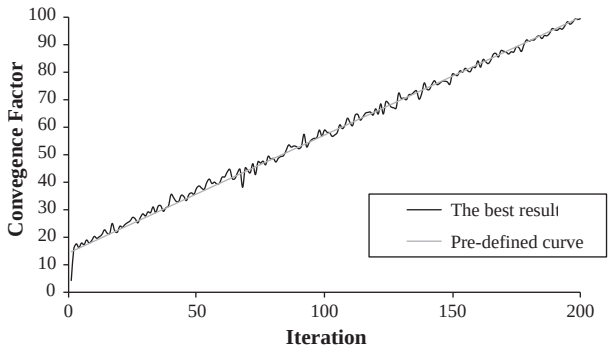

Fig. 31. The optimum answer and the average answer with the convergence factor history for the 3-bay 24-story planar frame using the DE.

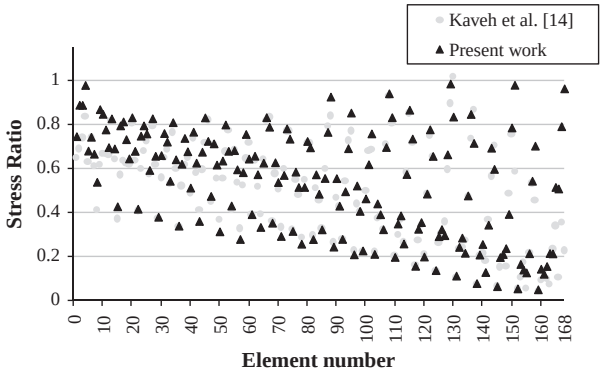

Fig. 30. Comparison of the allowable and existing stress ratio for the 3-bay 24-story planar frame.

sidering $PP_1 = 0.15$ and *Power* = 1. R_e and ε are equal to 5 and 1, respectively.

Results of the present study and those of Camp et al. [32], Degertekin [33] and Kaveh and Talatahari [34,31,14] are provided in Table 11. It can be seen that the DE achieves results that are 7.5%, 4.8%, 6%, 3.7%, and 3.6% lighter than those of the ACO, HS, IACO, ICA and CSS, respectively.

Convergence history is depicted in Fig. 28. It can be observed that DE leads to the best answer in 200 loops which is less than that of CSS being 275 loops.

The maximum value of displacement is 26.11 cm which is less than the allowable limit (29.20 cm).

Fig. 29 shows the inter-story drifts with maximum value being 1.202 cm that is less than the allowable value (1.205 cm). It can be recognized that by reducing the weight of structure its stiffness is reduced and the inter-story drifts are quite close to the maximum allowable value.

In Fig. 30 the stress ratios of the elements are shown. One can see that similar to the inter-story limitation, the stress ratios are closer to the limitation line. The maximum stress ratio is 98.33%.

Fig. 31 shows the *CF* changes during the optimization process. It is clear that the *CF* changes around the predefined line.

6. Conclusion

In this study a novel optimization method is developed based on dolphin echolocation. The new method has the advantage of working according to the computational effort that user can afford for his/her optimization. In this algorithm, the convergence factor defined by Kaveh and Farhoudi [1] is controlled in order to perform a suitable optimization.

For the examples optimized in this paper, the DE achieves better results with higher convergence rates compared to other existing meta-heuristic algorithms such as GA, ACO, PSO, BB–BC, HS, ESs, SGA, TS, ICA, IACO, PSOPC, HPSACO and CSS previously applied to these problems. The authors believe that the results achieved from meta-heuristics are mostly dependent on the parameter tuning of the algorithms. It is also believed that by performing a limited number of numerical examples, one cannot correctly conclude the superiority of one method with respect to the others. Dolphin echolocation is an optimization algorithm that has the capability of adopting itself by the type of the problem in hand, having a reasonable convergence rate, and leading to an acceptable optimum answer in a number of loops specified by the user.

Acknowledgements

The first author is grateful to the Iran National Science Foundation for the support.

References

[1] Kaveh A, Farhoudi N. A unified approach to parameter selection in meta-heuristic algorithms for layout optimization. J Constr Steel Res 2011;67:15453–62.
[2] Holland JH. Adaptation in natural and artificial systems. Ann Arbor: University of Michigan Press; 1975.
[3] Goldberg DE. Genetic algorithms in search optimization and machine learning. Boston: Addison-Wesley; 1989.
[4] Eberhart RC, Kennedy J. A new optimizer using particle swarm theory. In: Proceedings of the sixth international symposium on micro machine and human science, Nagoya, Japan; 1995.
[5] Gomes HM. Truss optimization with dynamic constraints using a particle swarm algorithm. Expert Syst Appl 2011;38:957–68.
[6] Dorigo M, Maniezzo V, Colorni A. The ant system: optimization by a colony of cooperating agents. IEEE Trans Syst Man Cybern 1996;B26(1):29–41.
[7] Kirkpatrick S, Gelatt C, Vecchi M. Optimization by simulated annealing. Science 1983;220:671–80.
[8] Geem ZW, Kim JH, Loganathan GV. A new heuristic optimization algorithm; harmony search. Simulation 2001;76:60–8.
[9] Rashedi E, Nezamabadi-pour H, Saryazdi S. GSA: a gravitational search algorithm. Inform Sci 2009;179:2232–48.
[10] Erol OK, Eksin I. New optimization method: Big Bang–Big Crunch. Adv Eng Softw 2006;37:106–11.
[11] Kaveh A, Talatahari S. Size optimization of space trusses using Big Bang–Big Crunch algorithm. Comput Struct 2009;87:1129–40.
[12] Kaveh A, Talatahari S. Particle swarm optimizer, ant colony strategy and harmony search scheme hybridized for optimization of truss structures. Comput Struct 2009;87:267–83.
[13] Kaveh A, Talatahari S. Optimization of large-scale truss structures using modified charged system search. Int J Optim Civil Eng 2011;1:15–28.
[14] Kaveh A, Talatahari S. Charged system search for optimal design of planar frame structures. Appl Soft Comput 2012;12:382–93.
[15] Kaveh A, Laknejadi K, Alinejad B. Performance based multi-objective optimization of large steel structures. Acta Mech 2012;223:355–69.
[16] Kaveh A, Talatahari S. A novel heuristic optimization method: charged system search. Acta Mech 2010;213:267–86.
[17] Yang XS. A new metaheuristic bat-inspired algorithm. NICSO 2010;284: 65–74.
[18] Griffin DR. Listening in the dark: the acoustic orientation of bats and men. New Haven (CT), Cambridge (MA): Yale University Press, Biological Laboratories, Harvard University; 1958. p. 413.
[19] Au WWL. The sonar of dolphins. New York: Springer; 1993.
[20] May J. The greenpeace book of dolphins. Greenpeace Communications Ltd.; 1990.
[21] Thomas JA, Moss CF, Vater M. Echolocation in bats and dolphins. University of Chicago Press; 2002.
[22] Wu SJ, Chow PT. Steady-state genetic algorithms for discrete optimization of trusses. Comput Struct 1995;56:979–91.
[23] Lee KS, Geem ZW, Lee SH, Bae KW. The harmony search heuristic algorithm for discrete structural optimization. Eng Optim 2005;37:663–84.
[24] Li LJ, Huang ZB, Liu F. A heuristic particle swarm optimization method for truss structures with discrete variables. Comput Struct 2009;87:435–43.
[25] Kaveh A, Talatahari S. A particle swarm ant colony optimization for truss structures with discrete variables. Comput Struct 2009;87:1129–40.
[26] Construction (AISC). Manual of steel construction allowable stress design, 9th ed., Chicago (IL); 1989.
[27] Hasançebi O, Çarbaş S, Doğan E, Erdal F, Saka MP. Performance evaluation of metaheuristic search techniques in the optimum design of real size pin jointed structures. Comput Struct 2009;87(5–6):284–302.
[28] ANSI/AISC 360-05. Specification for structural steel buildings. Chicago, Illinois 60601-1802: American Institute of Steel Construction, March 9; 2005.
[29] Kaveh A, Talatahari S. Hybrid algorithm of harmony search, particle swarm and ant colony for structural design optimization. Stud Comput Intell 2009;239:159–98.
[30] Sonmez M. Discrete optimum design of truss structures using artificial bee colony algorithm. Struct Multidisc Optim 2011;43:85–97.
[31] Kaveh A, Talatahari S. Optimum design of skeletal structures using imperialist competitive algorithm. Comput Struct 2010;88:1220–9.
[32] Camp CV, Bichon J, Stovall SP. Design of steel frames using ant colony optimization. J Struct Eng – ASCE 2005;131(3):369–79.
[33] Degertekin SO. Optimum design of steel frames using harmony search algorithm. Struct Multidiscip Optim 2008;36:393–401.
[34] Kaveh A, Talatahari S. An improved ant colony optimization for design of planar steel frames. Eng Struct 2010;32:864–76.